



Multiple hysteretic patterns from elementary population models

Theresa Wei Ying Ong^{1,2} · John Vandermeer²

Received: 28 September 2017 / Accepted: 9 April 2018 / Published online: 21 April 2018
© Springer Science+Business Media B.V., part of Springer Nature 2018

Abstract

Critical transitions whereby small changes in conditions can cause large and irreversible changes in ecosystem states are a cause of increasing concern in ecology. Here, we focus on the irreversibility of these transitions, formally known as hysteresis. We explore how simple correlations between parameters in Lotka-Volterra predator-prey equations result in a variety of complicated hysteretic patterns. These patterns include “unattainable” stable states that once lost may never be recovered. We suspect these patterns to be common in natural systems, where interactions between diverse assemblages are unavoidable. Thus, understanding underlying hysteretic structures may be necessary for rescuing lost ecosystem states and avoiding future losses.

Keywords Hysteresis · Tipping points · Critical transitions · Predator-prey models · Unattainable states · Complexity

Introduction

Tipping points, also called critical transitions, are increasingly acknowledged as important elements of ecological systems (Scheffer 2009; Scheffer et al. 2012). They emerge in popular perception as potential doomsday behemoths in the context of climate change research where multiple tipping points may form a perfect doomsday storm: arctic ice melts to the point where the previous moderating albedo effect is lost, atmospheric heat rises suddenly above the point where methane hydrate currently sequestered in permafrost begins runaway melting; two critical transitions that push the system past a third sudden drop in the Atlantic thermohaline circulation, which may in turn drive collapse in other ecosystems (Kvenvolden 1988; Lenton 2011; Hughes et al. 2013). Many other examples could be cited (May 1977; Vandermeer et al. 2004; Scheffer 2009). Many critical transitions involve hysteresis, an associated structure in which movement of a control parameter in one direction generates a tipping point that is

distinct from a tipping point when the control parameter is moved in the opposite direction. Thus, reducing rainfall in the Amazon may generate, at some critical threshold of rainfall, a dramatic switch from forest to savannah, but having undergone that switch, increasing the rainfall to where it had been before, will not necessarily result in regeneration of the forest (Hirota et al. 2011; Staver et al. 2011).

The importance of hysteresis is evident in many practical situations (fisheries management, pest management, forestry, coral reefs, lake eutrophication) (Knowlton 1992; Huang et al. 1998; Carpenter et al. 1999; Mumby and Hastings 2008; Petrie et al. 2009; Elmhirst et al. 2009; Ong and Vandermeer 2015). Research in this area has documented loss of resilience and biodiversity in many ecosystems and has yielded important predictions on when tipping points are expected and how systems may be managed to reduce vulnerability of collapse (Folke et al. 2010). The idea of hysteresis is not unusual, effectively recognized since the recognition of alternative stable equilibria in, for example, the Gaussian concept of indeterminate competition or many other classical ecological applications (May 1977). Yet the current ecological literature on the topic has focused almost entirely on a single form of hysteresis, a saddle-node bifurcation. This classic S-curve form is generated from systems where two stable equilibria are separated by a single unstable center. The saddle-node bifurcation occurs when one of the stable equilibria collides with the unstable to eliminate each other, leaving one remaining stable equilibrium (Strogatz 2001; Scheffer 2009). Switching between the two stable equilibria is driven by a change in some

✉ Theresa Wei Ying Ong
wyong@princeton.edu

¹ Department of Ecology and Evolutionary Biology, Princeton University, M31 Guyot Hall, Princeton, NJ 08544, USA

² Department of Ecology and Evolutionary Biology, University of Michigan, 830 North University, Kraus Natural Science Building, Ann Arbor, MI 48109, USA

(usually human-induced) variable, for example, harvest rates in fisheries or nutrient input rates in lakes (Carpenter et al. 1999; Schröder et al. 2005; Petrie et al. 2009). Though authors acknowledge that many variables within a single system are capable of driving critical transitions, the effects of multiple driver variables on patterns of hysteresis remain unexplored (Wang et al. 2012; Möllmann et al. 2015; Rocha et al. 2015). While we commonly acknowledge a variety of dynamical concepts potentially involved in community structure (e.g., multiple dimensions, stable/unstable points and cycles, chaos, deterministic versus stochastic forces, time lags), the possibility that hysteresis itself may be complicated is less frequently acknowledged and, we argue, worthy of consideration. Here, we consider how correlations between multiple driver variables influence hysteresis, demonstrating that the hysteretic patterns of a common form of the Lotka-Volterra predator-prey equations can be diverse and complicated.

Theoretical approach

We begin with the classic equations and then add two popular nonlinearities. The key nonlinearities normally added are (1) density dependence on the prey (resource, host) element and (2) a functional response (satiation) on the predatory element. Adding density dependence to the prey and predator satiation, the resultant equations are:

$$\frac{dV}{dt} = rV(1-V) - \frac{\alpha VP}{1 + \beta V} \tag{1a}$$

$$\frac{dP}{dt} = \frac{\delta VP}{1 + \beta V} - mP \tag{1b}$$

where r is the prey (V) growth rate, α is the predator (P) attack rate, β is the saturation constant of the predator, δ is the conversion rate of prey to predators, and m is the predator mortality rate. The classic picture in phase space as pioneered by Rosenzweig and MacArthur (1963) is illustrated in Fig. 1.

Relaxing the assumption that the predator is limited only by its prey (i.e., allowing for there to be density-dependent control on the predator as well as the prey), several authors have analyzed the more complicated possibilities that may emerge (Noy-Meir 1975; Vandermeer and King 2010). For example, adding a carrying capacity k to the predator transforms system 2 into:

$$\frac{dV}{dt} = rV(1-V) - \frac{\alpha VP}{1 + \beta V} \tag{2a}$$

$$\frac{dP}{dt} = \frac{\delta VP}{1 + \beta V} \left(1 - \frac{P}{k}\right) - mP \tag{2b}$$

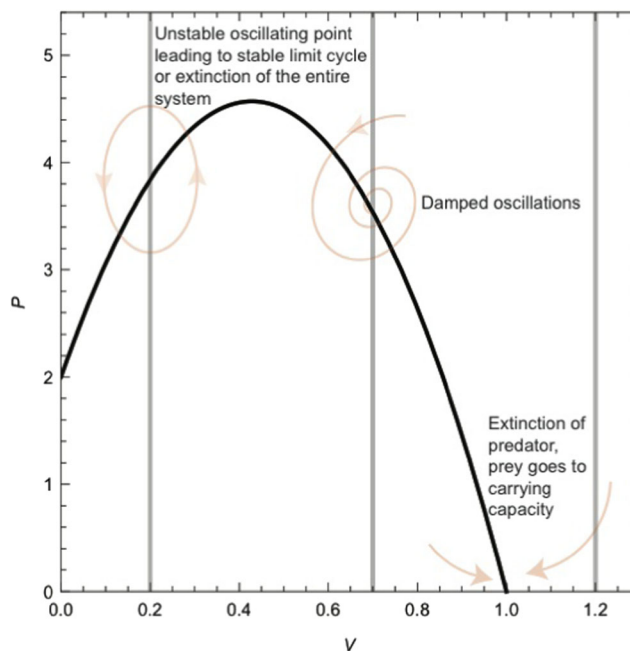


Fig. 1 Classic phase space representation of a predator-prey system, illustrated by the combination of predator (P , gray lines) and prey (V , black line) zero growth isoclines. The placement of the predator isocline stipulates which of the three dynamic outcomes results. Pink arrows indicate dynamic trajectories

with zero growth isoclines:

$$P = \frac{r(1-V)(1 + \beta V)}{\alpha} \tag{3a}$$

$$P = \frac{k(\delta V - \beta m V - m)}{\delta V} \tag{3b}$$

Here, as proposed qualitatively by Noy-Meir in 1975 and Rosenzweig and MacArthur in 1963, if the predator has an independent source of control, this places a cap on the predator isocline and creates conditions for alternative equilibrium points, including bifurcation patterns that suggest the system may respond in a critical transition fashion to a variety of parameter manipulations, as demonstrated in Fig. 2. Most notable is the zone of hysteresis, suggesting different meta-behavior of the system as the parameter is varied (indicated by dashed arrows). If the predator carrying capacity is high (say around 7 in Fig. 2a), the equilibrium of the prey is low. As we reduce the carrying capacity of the predator, the equilibrium of the prey remains relatively low, until we decrease the carrying capacity to the critical point (about 4.6 in Fig. 2a), and the prey equilibrium density jumps up dramatically. Reversing the tuning of k , the prey equilibrium begins to decline, but reaches a critical point at a value of k that is larger than the original critical point, thus creating a zone of hysteresis, within which alternative stable situations coexist.

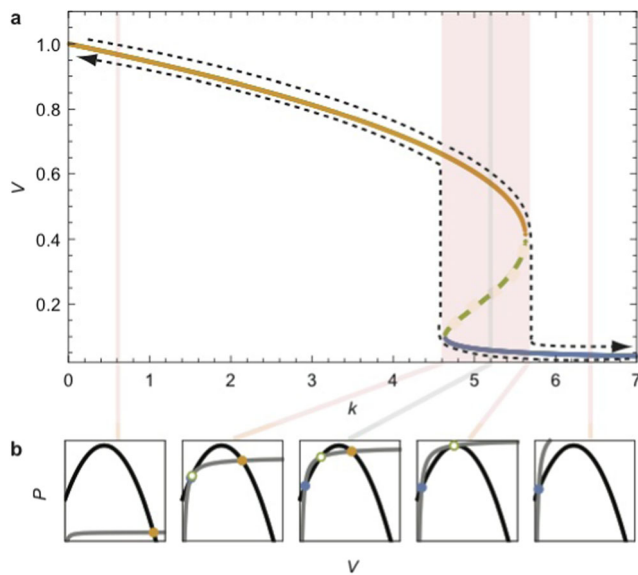


Fig. 2 Changing upper-limited predator isocline in **b**, illustrating tipping point behavior and zone of hysteresis in **a**. Dashed arrows in **a** indicate distinct behavior associated with reducing k from high to low versus increasing k from low to high. Shaded area is zone of hysteresis. Stable equilibrium points plotted in orange and blue, along with unstable green points (dotted line). Lines connect equilibrium point in graph **a** to its corresponding isocline arrangement in **b**

The equilibrium points are given as the roots to the equation,

$$\frac{r(1-V)(1 + \beta V)}{\alpha} = \frac{k(\delta V - \beta m V - m)}{\delta V} \quad (4)$$

or

$$\alpha k m + (r\delta - \alpha k \delta + \alpha k \beta m)V + r\delta(\beta - 1)V^2 - r\delta\beta V^3 = 0 \quad (5)$$

which has roots $\lambda_1, \lambda_2,$ and λ_3 (in order of size). The points of critical transition are then $[\lambda_3 > \lambda_1 = \lambda_2]$ and $[\lambda_1 < \lambda_2 = \lambda_3]$, as illustrated in panels 2 and 4 of Fig. 2b.

In reality, it is unlikely that effects of an environmental change will be restricted to a single parameter (as in Fig. 2 where the carrying capacity of the predator is the only change resulting from change in a postulated environmental driver). Most frequently, parameters are likely to change in a correlated fashion. They may be positive: planting more shade trees in a coffee farm is likely to positively influence both the growth rate and carrying capacity of arboreal ants (Perfecto and Vandermeer 2015); negative: increasing the nitrogen input of lakes may increase phytoplankton growth rates (Howarth and Cole 1985), but decrease their carrying capacity as dissolved oxygen becomes limited (Foley et al. 2012); and more often than not, nonlinear: introduction of cane toads may at first reduce the carrying capacity of cane beetles, but biological control becomes ineffective when cane toads outcompete native anurans and switch diets to native, nontarget invertebrate

prey, causing an overall convex relationship between cane toad attack rates and cane beetle carrying capacity (Shine 2010). While many parameters in our proposed model may exhibit correlated changes (discussed below), our intent in this article is simply to illustrate the qualitatively rich hysteretic behavior of this elementary pair of equations. Thus, we focus on correlations between predator attack rate (α) and the predator carrying capacity (k), a combination that generates a rich diversity of critical transition behaviors.

Methods

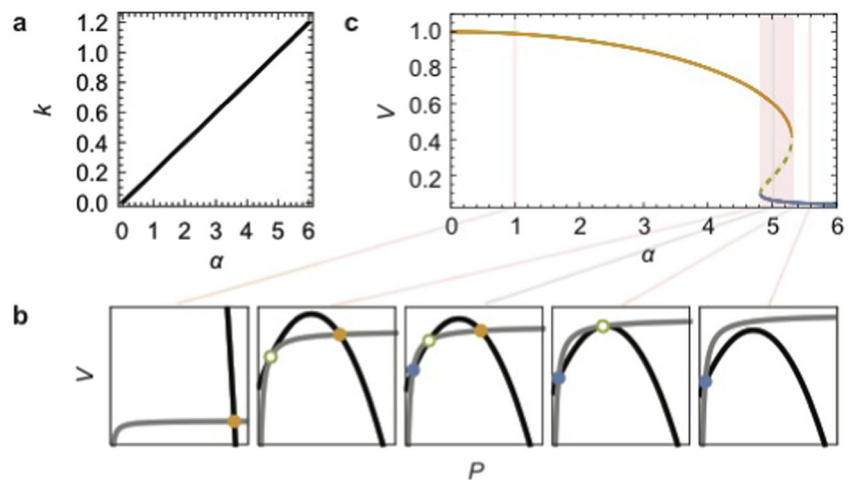
To observe hysteretic patterns resulting from Eq. 2a to 2b, we analytically calculated three unique equilibrium points from the intersection of predator and prey isoclines. Equilibrium points were plotted as a function of driver variables α and k using a variety of theoretical correlations between the two parameters (linear, parabolic, and polynomial). The functions are listed in Fig. 4. Analytical solutions for critical points were impossible because of the higher order nature of equilibrium point equations; thus, critical points were determined using a numerical approach, testing for equality in equilibrium points as a function of 0.01 interval changes in the driver variable α . To demonstrate how these patterns emerge, we plot three-dimensional plots of prey population equilibria as a function of α and k . We run cross-sections through 3D plots holding either α or k constant as well as cross-sections where α and k are correlated. Hysteretic patterns from correlating other parameters in the model (r, δ, β, m) are also assessed.

Results

In Fig. 3, we illustrate the situation in which the variation in k and α is such that they are positively correlated. Qualitatively, the tipping point behavior is identical to the previous example (Fig. 2), although the details are distinct (note that both isoclines change along with simultaneous changes in k and α).

In Fig. 4, we illustrate four other potential correlations in the simultaneous response of k and α to some environmental driver. Note how the patterns of hysteresis can become quite complicated. In particular, in Fig. 4a, b, we show the mirror results of an environmental change that changes k and α proportionally (linearly) (Fig. 4a is a repeat of Fig. 3). In Fig. 4c, the relationship between α and k is somewhat more complicated, but the resulting hysteretic zones can be easily predicted from the hysteretic patterns of Fig. 4a, b separately. Yet the pattern itself suggests the existence of a complicated relationship between the tuning variable and the resulting equilibrium points. Sudden loss of the prey population is eventually replaced with sudden gain, even as the tuning parameter is changed in the same direction. For example, if the classic

Fig. 3 Expected pattern of critical transitions and hysteretic zone when predator attack rate (α) and carrying capacity (k) are positively correlated. **a** Plot of variable α against variable k for the values used in the calculations. **b** Five exemplary isocline arrangements as k and α are varied. **c** Resulting critical transition and hysteretic zone (shaded) for the system (qualitatively the same as Fig. 2). Stable equilibrium points plotted in orange and blue, along with unstable green points (dotted line)



enrichment approach were to be applied to a predator destined to be a biological control agent, initially, we might imagine an increase in both k and α as the enrichment program favored many aspects of the predator's niche. However, it is conceivable that as the program moves forward, the connection between the carrying capacity (k) and the attack rate (α) may break down. It is likely that consumption efficiency decreases once attack rate (α) surpasses a critical threshold. The lower consumption efficiency, extra search time, and aggression associated with extremely high attack rates could pull down carrying capacity, producing a hump-shaped relationship between α and k whence the hysteresis pattern of Fig. 4c emerges. The prey item thus would go from very high (which, if a potential pest species, for example, would be detrimental) to virtual extinction in response to the enrichment program. Yet further enrichment would surprisingly produce yet again a burgeoning prey population. At any time, reversing course would result in tipping points again, but at relatively unpredictable points in the enrichment program.

The example in Fig. 4d presents a qualitatively distinct picture, in which a locus of stable points may be unreachable. Once the system is at the lower equilibrium point, there is no way to reach the stable locus through the tuning parameter. If the system starts within the stable set, it will remain there, but only through a narrow range of tuning parameter values. Once it reaches a tipping point, the prey population descends to almost zero and is unable to reach the stable situation ever again. The conservation implications here are evident. If the prey species is of conservation concern, and efforts are made to either decrease or increase the predatory influence on it, the result could be a critical transition to a very low population density, which may become stagnated at that point no matter what future manipulations may be undertaken.

In Fig. 4e, we illustrate what is effectively a combination of the situations in Fig. 4c, d. Again, there is an “unattainable” locus of equilibrium points. But here, we have three distinct hysteretic zones, from very high prey at one end of the tuning

parameter to very high at the other end, with two hysteretic zones in between, but also including a hysteretic zone at the locus of the “unattainable” points. If, for whatever reason, the intermediate density is the desired one, as in the example in Fig. 4d, it could easily be lost to the larger densities at either low or high tuning parameter values, never to return again because of the nature of the intermediate hysteretic zone.

To demonstrate how these patterns emerge, we plot a three-dimensional plot of the three unique equilibria as a function of k and α (Fig. 5). As mentioned earlier, independent changes to either k or α can cause hysteresis. Thus, cross-sections along the k or α direction reveal the classic S-curve hysteretic form, a saddle-node bifurcation (Fig. 5a). Simultaneously plotting both k and α cross-sections reveals how complicated hysteretic patterns emerge (Fig. 5b). Merging of two independent saddle-node bifurcations creates the potential for double hysteretic loops and hidden loops as those cross-sections collide when parameters are correlated (Fig. 5b, c). This simple graphical analysis illustrates the generality of these patterns. Any two parameters capable of independently causing hysteresis in the model should also be capable of generating more complicated hysteretic patterns when they are correlated in an appropriate fashion. We illustrate this in Fig. 5d, e by bifurcating the remaining parameters (r , δ , β , m) against each other. In Fig. 5f, cross-sections of a cusp bifurcation (where hysteresis along one axis is gradually lost) show how the potential for complicated hysteretic patterns disappear as the second saddle-node bifurcation disappears at around 8 on the α axis (Thom 1969).

Discussion

The literature on tipping points in ecology is large (Schröder et al. 2005; Scheffer 2009; Scheffer et al. 2012), but the associated issue of hysteresis has remained constrained to a simple saddle-node form thus far. From both a basic structural phenomenon and a practical standpoint, hysteresis is an important

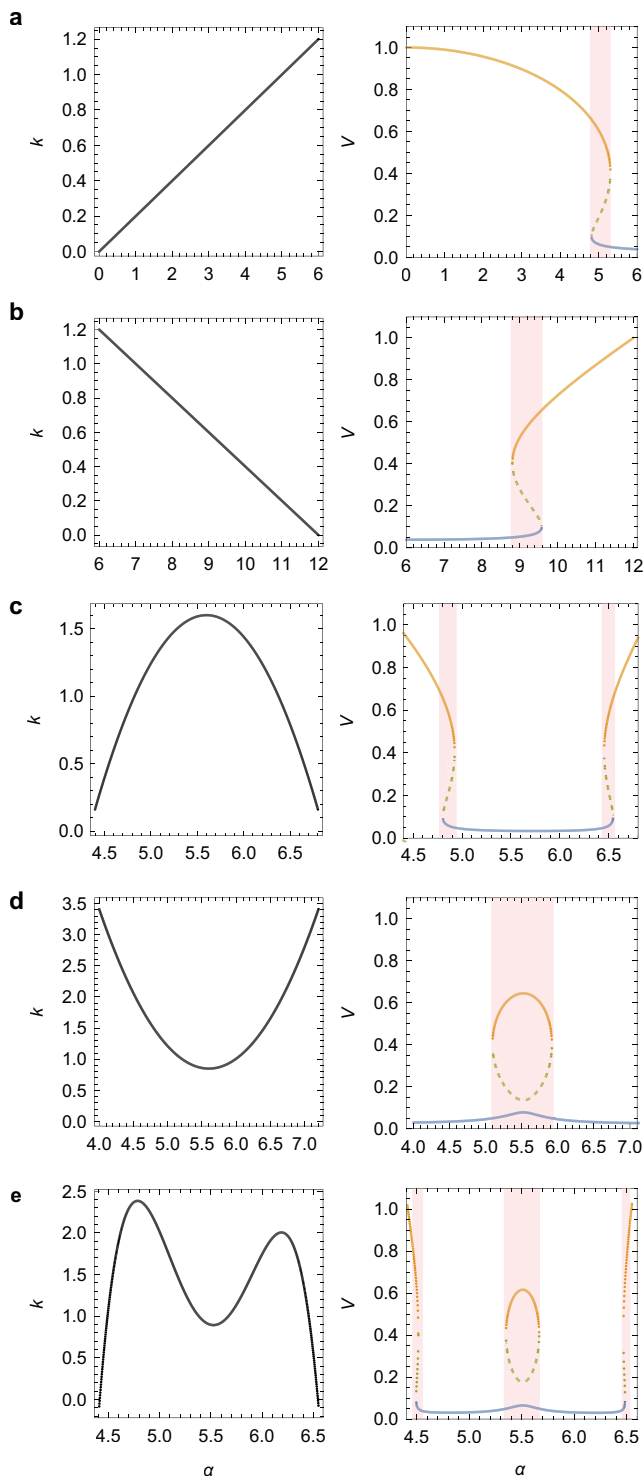


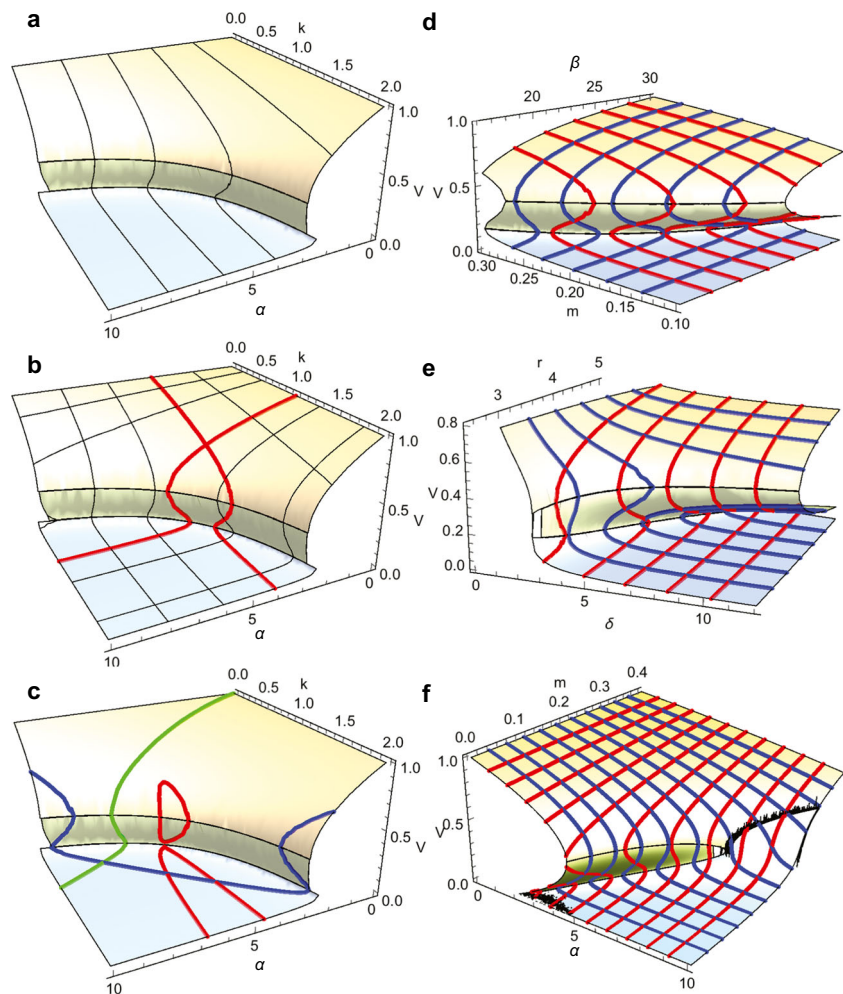
Fig. 4 A menagerie of hysteretic patterns. Examples of **a–b** linear, parabolic **c–d** and **e** polynomial correlations between the tuning parameter α and k , and resulting hysteretic patterns. Equations for correlations between α and k are **a** $k = 0.2\alpha$, **b** $k = -0.2\alpha + 2.4$, **c** $k = -(\alpha - 5.6)^2 + 1.6$, **d** $k = (\alpha - 5.6)^2 + 0.85$, **e** $k = -5.3335\alpha^4 + 117.331\alpha^3 - 962.671\alpha^2 + 3490.77\alpha - 4718$, and critical transition points for hysteretic regions are $\alpha_c =$ **a** 4.81, 5.31; **b** 8.80, 9.58; **c** 4.80, 4.93, 6.45, 6.55; **d** 5.10, 5.92; and **e** 4.49, 4.51, 5.35, 5.67, 6.47, 6.48. Stable equilibrium points plotted in orange and blue, along with unstable green points (dotted line). Red shaded region is zone of hysteresis

force. Especially in any form of environmental management, it is perhaps disheartening to learn that errors in management decisions are not easily reversible. Historical examples abound. For example, a change in fishing technology that increases harvesting of the top predator, cod, can switch the ecosystem to one dominated by herring (Fauchald 2010), but a subsequent reversal of that change will not necessarily result in the reversion to a healthy cod population. A decision to eliminate shade trees from a coffee plantation encourages weedy growth and the inevitable competition from weeds, yet returning to shade is impossible since those weeds compete with newly planted tree seedlings (Perfecto and Vandermeer 2015). Beyond management considerations, tipping points are well known to contextualize larger ecosystems, at least theoretically (Vandermeer and Yodzis 1999; Schreiber 2003; Scheffer et al. 2012). Since it is frequently the case that tipping points carry with them hysteresis, it would be prudent to ask what effect such behavior will have when embedded in larger systems (Giller et al. 1997; Merton 1998; van Nes and Scheffer 2004).

Positive, negative, and nonlinear relationships between predator attack rates and carrying capacities are simple examples of a large number of possibilities in the full parameter or life history trait space of a complex community. Some ecological systems exhibit strong negative density dependence, while other populations grow best when larger (Allee et al. 1949; Courchamp et al. 1999; Brook and Bradshaw 2006). Both are common ecological patterns that can conceivably result in the negative and positive relationships between attack rates and carrying capacity presented here (Fig. 4a, b). Often, there is some combination of positive and negative density dependence that combines to create nonlinear relationships (Comita et al. 2010). Concave patterns can result from Allee effects where cooperation is important for small populations, but gives way to intraspecific competition at high densities (Fig. 4c) (Allee et al. 1949; Courchamp et al. 1999). Convex patterns may occur when diseases spread or natural enemies are attracted only after targeted populations exceed critical thresholds (Janzen 1970; Connell 1971; Anderson and May 1979; Berryman 1982). However, once these populations are sufficiently large, herd immunity can restore population sizes resulting in the convex shape in Fig. 4d that leads to hidden stable states (Magurran 1990; Anderson and May 1990). Many more possibilities can be imagined and combined to create more complex nonlinearities like in Fig. 4e.

We have shown that complex hysteretic patterns very easily emerge from simple correlations between parameters in classic Lotka-Volterra population models. These complexities are likely the rule, not exception, for larger systems, where higher order interactions much exceeding the simple correlations explored here, abound. In basic hysteresis, changes to the state of an ecosystem are merely difficult to reverse; decreases in global precipitation may transform forests into

Fig. 5 Three-dimensional graphical analysis of complex hysteretic patterns. Plots of 3 unique equilibria for prey (V) in Lotka-Volterra model, 2 stable (orange and blue regions), and 1 unstable (green regions) as a function of model parameters. In **a**, cross-sections are drawn along k (predator carrying capacity) axis. In **b**, cross-sections are drawn along both the k and α (predator attack rate) axes, with one cross-section in each axis highlighted in red. In **c**, cross-sections with positive (green), concave (blue), and convex parabolic (red) correlations between k and α are drawn. Plots of pest equilibria as a function of remaining model parameters **d** predator satiation (β) and predator mortality (m), and also **e** prey growth rate (r) and predator conversion rate (δ). An example of a cusp bifurcation in **f**. Red and blue lines correspond to cross-sections along each respective axis in **d–f**



savannahs, and if the rain were to suddenly increase, forests may still not return for many years (Staver et al. 2011). But if the hysteretic patterns are such that the forest state is “unattainable,” reversion to forests may be impossible once a transition to savannahs has occurred. Reversion to the pre-transition state is indeed impossible if management focuses only on the drivers of change (in our last example, precipitation or for management purposes, irrigation). It is, however, conceivable to reach the “unattainable” state through an external perturbation that shifts the ecosystem state itself. In the last example, precipitation may drive changes in the ecosystem state, but rather than adding water to the system, managers could instead restore forest plants to artificially shift the ecosystem state while precipitation remains constant. Yet restoring the forest would in theory be unsuccessful if the system was not situated at the precipitation level where the “unattainable” forest state could be achieved by a vertical shift in the ecosystem state. In such cases, successful reversion to ideal states depends strongly on how well the underlying hysteretic nature of the system is understood. Since complex hysteretic patterns are likely commonplace in nature, we suggest

that studies focused on characterizing patterns of hysteresis are essential for both rescuing systems that have transitioned to undesirable states and preventing unwanted transitions from occurring in the first place.

Acknowledgements We would like to thank Gyuri Barabas for the help with numerical approximations of critical transition points.

Funding information This study was funded by the Ecology and Evolutionary Biology Department and the Rackham Graduate School at the University of Michigan.

References

- Allee WC, Park O, Emerson AE et al (1949) Principles of animal ecology. Princ Anim Ecol
- Anderson RM, May RM (1979) Population biology of infectious diseases: part I. Nature 280:361–367
- Anderson RM, May RM (1990) Immunisation and herd immunity. Lancet 335:641–645. [https://doi.org/10.1016/0140-6736\(90\)90420-A](https://doi.org/10.1016/0140-6736(90)90420-A)

- Berryman AA (1982) Biological control, thresholds, and pest outbreaks. *Environ Entomol* 11:544–549. <https://doi.org/10.1093/ee/11.3.544>
- Brook BW, Bradshaw CJA (2006) Strength of evidence for density dependence in abundance time series of 1198 species. *Ecology* 87:1445–1451. [https://doi.org/10.1890/0012-9658\(2006\)87\[1445:SOEFDD\]2.0.CO;2](https://doi.org/10.1890/0012-9658(2006)87[1445:SOEFDD]2.0.CO;2)
- Carpenter SR, Ludwig D, Brock WA (1999) Management of eutrophication for lakes subject to potentially irreversible change. *Ecol Appl* 9:751–771. [https://doi.org/10.1890/1051-0761\(1999\)009\[0751:MOEFLS\]2.0.CO;2](https://doi.org/10.1890/1051-0761(1999)009[0751:MOEFLS]2.0.CO;2)
- Comita LS, Muller-Landau HC, Aguilar S, Hubbell SP (2010) Asymmetric density dependence shapes species abundances in a tropical tree community. *Science* 329:330–332. <https://doi.org/10.1126/science.1190772>
- Connell J (1971) On the role of natural enemies in preventing competitive exclusion in some marine animals and in rain forest trees. In: *Dynamics of populations*. Center for Agricultural Publication and Documentation
- Courchamp F, Clutton-Brock T, Grenfell B (1999) Inverse density dependence and the Allee effect. *Trends Ecol Evol* 14:405–410. [https://doi.org/10.1016/S0169-5347\(99\)01683-3](https://doi.org/10.1016/S0169-5347(99)01683-3)
- Elmhirst T, Connolly SR, Hughes TP (2009) Connectivity, regime shifts and the resilience of coral reefs. *Coral Reefs* 28:949–957. <https://doi.org/10.1007/s00338-009-0530-8>
- Fauchald P (2010) Predator–prey reversal: a possible mechanism for ecosystem hysteresis in the North Sea? *Ecology* 91:2191–2197. <https://doi.org/10.1890/09-1500.1>
- Foley B, Jones ID, Maberly SC, Rippey B (2012) Long-term changes in oxygen depletion in a small temperate lake: effects of climate change and eutrophication. *Freshw Biol* 57:278–289. <https://doi.org/10.1111/j.1365-2427.2011.02662.x>
- Folke C, Carpenter SR, Walker B et al (2010) Resilience thinking: integrating resilience, adaptability and transformability. *Ecol Soc* 15:20
- Giller KE, Beare MH, Lavelle P, Izac AMN, Swift MJ (1997) Agricultural intensification, soil biodiversity and agroecosystem function. *Appl Soil Ecol* 6:3–16. [https://doi.org/10.1016/S0929-1393\(96\)00149-7](https://doi.org/10.1016/S0929-1393(96)00149-7)
- Hirota M, Holmgren M, Van Nes EH, Scheffer M (2011) Global resilience of tropical forest and savanna to critical transitions. *Science* 334:232–235
- Howarth RW, Cole JJ (1985) Molybdenum availability, nitrogen limitation, and phytoplankton growth in natural waters. *Science* 229:653–655. <https://doi.org/10.1126/science.229.4714.653>
- Huang W, Yu H, Weber WJ Jr (1998) Hysteresis in the sorption and desorption of hydrophobic organic contaminants by soils and sediments: 1. A comparative analysis of experimental protocols. *J Contam Hydrol* 31:129–148. [https://doi.org/10.1016/S0169-7722\(97\)00056-9](https://doi.org/10.1016/S0169-7722(97)00056-9)
- Hughes TP, Carpenter S, Rockström J, Scheffer M, Walker B (2013) Multiscale regime shifts and planetary boundaries. *Trends Ecol Evol* 28:389–395. <https://doi.org/10.1016/j.tree.2013.05.019>
- Janzen DH (1970) Herbivores and the number of tree species in tropical forests. *Am Nat* 104:501–528. <https://doi.org/10.1086/282687>
- Knowlton N (1992) Thresholds and multiple stable states in coral reef community dynamics. *Integr Comp Biol* 32:674–682. <https://doi.org/10.1093/icb/32.6.674>
- Kvenvolden KA (1988) Methane hydrate—a major reservoir of carbon in the shallow geosphere? *Chem Geol* 71:41–51
- Lenton TM (2011) Early warning of climate tipping points. *Nat Clim Chang* 1:201–209
- Magurran AE (1990) The adaptive significance of schooling as an anti-predator defence in fish. *Ann Zool Fenn* 27:51–66
- May RM (1977) Thresholds and breakpoints in ecosystems with a multiplicity of stable states. *Nature* 269:471–477
- Merton R (1998) Monitoring community hysteresis using spectral shift analysis and the red-edge vegetation stress index. pp 12–16
- Möllmann C, Folke C, Edwards M, Conversi A (2015) Marine regime shifts around the globe: theory, drivers and impacts. *Phil Trans R Soc B* 370:20130260. <https://doi.org/10.1098/rstb.2013.0260>
- Mumby PJ, Hastings A (2008) The impact of ecosystem connectivity on coral reef resilience. *J Appl Ecol* 45:854–862. <https://doi.org/10.1111/j.1365-2664.2008.01459.x>
- Noy-Meir I (1975) Stability of grazing systems: an application of predator-prey graphs. *J Ecol* 63:459–481. <https://doi.org/10.2307/2258730>
- Ong TW, Vandermeer JH (2015) Coupling unstable agents in biological control. *Nat Commun* 6
- Perfecto I, Vandermeer J (2015) Coffee agroecology: a new approach to understanding agricultural biodiversity, ecosystem services and sustainable development. Routledge
- Petrie B, Frank KT, Shackell NL, Leggett WC (2009) Structure and stability in exploited marine fish communities: quantifying critical transitions. *Fish Oceanogr* 18:83–101. <https://doi.org/10.1111/j.1365-2419.2009.00500.x>
- Rocha J, Yletyinen J, Biggs R, Blenckner T, Peterson G (2015) Marine regime shifts: drivers and impacts on ecosystems services. *Phil Trans R Soc B* 370:20130273. <https://doi.org/10.1098/rstb.2013.0273>
- Rosenzweig ML, MacArthur RH (1963) Graphical representation and stability conditions of predator-prey interactions. *Am Nat* 97:209–223
- Scheffer M (2009) *Critical transitions in nature and society*. Princeton University Press
- Scheffer M, Carpenter SR, Lenton TM, Bascompte J, Brock W, Dakos V, van de Koppel J, van de Leemput IA, Levin SA, van Nes EH, Pascual M, Vandermeer J (2012) Anticipating critical transitions. *Science* 338:344–348. <https://doi.org/10.1126/science.1225244>
- Schreiber SJ (2003) Allee effects, extinctions, and chaotic transients in simple population models. *Theor Popul Biol* 64:201–209. [https://doi.org/10.1016/S0040-5809\(03\)00072-8](https://doi.org/10.1016/S0040-5809(03)00072-8)
- Schröder A, Persson L, De Roos AM (2005) Direct experimental evidence for alternative stable states: a review. *Oikos* 110:3–19. <https://doi.org/10.1111/j.0030-1299.2005.13962.x>
- Shine R (2010) The ecological impact of invasive cane toads (*Bufo marinus*) in Australia. *Q Rev Biol* 85:253–291. <https://doi.org/10.1086/655116>
- Staver AC, Archibald S, Levin SA (2011) The global extent and determinants of savanna and forest as alternative biome states. *Science* 334:230–232
- Strogatz S (2001) *Nonlinear dynamics and chaos: with applications to physics, biology, chemistry and engineering*. Perseus Books Group
- Thom R (1969) Topological models in biology. *Topology* 8 (3):313–335
- van Nes EH, Scheffer M (2004) Large species shifts triggered by small forces. *Am Nat* 164:255–266. <https://doi.org/10.1086/422204>
- Vandermeer J, Granzow de la Cerda I, Perfecto I et al (2004) Multiple basins of attraction in a tropical forest: evidence for nonequilibrium community structure. *Ecology* 85:575–579. <https://doi.org/10.1890/02-3140>
- Vandermeer J, King A (2010) Consequential classes of resources: subtle global bifurcation with dramatic ecological consequences in a simple population model. *J Theor Biol* 263:237–241. <https://doi.org/10.1016/j.jtbi.2009.12.006>
- Vandermeer J, Yodzis P (1999) Basin boundary collision as a model of discontinuous change in ecosystems. *Ecology* 80:1817–1827. [https://doi.org/10.1890/0012-9658\(1999\)080\[1817:BBCAAM\]2.0.CO;2](https://doi.org/10.1890/0012-9658(1999)080[1817:BBCAAM]2.0.CO;2)
- Wang R, Dearing JA, Langdon PG, Zhang E, Yang X, Dakos V, Scheffer M (2012) Flickering gives early warning signals of a critical transition to a eutrophic lake state. *Nature* 492:419–422. <https://doi.org/10.1038/nature11655>